

ON THE FORMATION AND DYNAMICS OF MASS-OUTFLUX FROM MATTER ACCRETING ONTO COMPACT OBJECTS

Tapas Kumar Das¹

¹ Theoretical Astrophysics Group
S. N. Bose National Centre For Basic Sciences
Calcutta 700 091 India
E-mail tdas@boson.bose.res.in

Active galaxies and quasars are believed to harbour Black Holes at their centers and at the same time produce cosmic radio jets through which immense amount of matter and energy are ejected out of the core of the galaxy. In our work we compute the mass outflow rates from advective accretion disks around black holes, which, in principal could explain the origin of jet formation in self-consistent manner. These computations are done using combinations of exact transonic inflow and outflow solutions which may or may not form shock waves. The approach of our calculation is somewhat different from that used in the literature so far. Our work for the first time connects the accretion type and wind type topologies self consistently. Our result, in general, matches with numerical simulation works and successfully points out to non-steady behavior which may evacuate the disk producing quiescence states.

Introduction

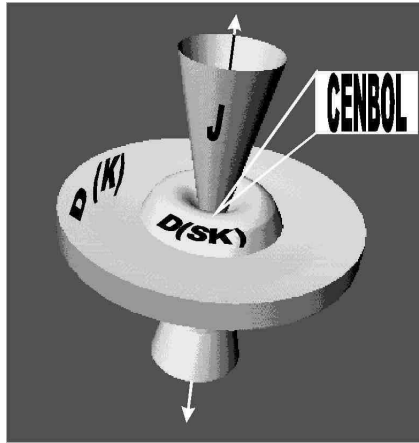
It is now widely believed that active galaxies and quasars harbour compact objects at their centres. One of the prominent signatures of activity around these objects is the generation of mass outflow in the form of jets. AGNs produce cosmic radio jets through which immense amount of matter and energy are spurted out of the core of the galaxies. Even the micro-quasars having stellar mass black holes at their centres have recently been discovered which exhibit same sort of phenomena. Sometime these outflows show superluminal motion also. The existing models in the present literature which study the formation and dynamics of mass outflow are roughly of three types. The first type of solutions confine themselves to the jet properties only, completely decoupled from the internal properties of accretion disks [1]. In the second type, efforts are made to correlate the internal structure of the accretion disks with that of the outflow using both hydrodynamics [2] and magnetohydrodynamics [3]. In the third type, numerical

simulations are carried out to observe how matter is being deflected from the equatorial plane towards the axis [4,5,6,7,8]. From the analytical front, although the wind type and the accretion type solutions come out from the same set of governing equations, there were no attempt to find connections among them. As a result, the computation of the outflow rate directly from the inflow parameters has always been impossible. Our work, *for the first time*, quantitatively connects the topologies of the inflow and the outflow to give a self consistent model for computing the mass loss rate from compact objects.

The mass outflow rates from the ordinary stellar bodies have been calculated very accurately from the stellar luminosity because theory of radiatively driven winds seems to be well understood [9]. The most fundamental difference between the mass loss from normal stellar objects and compact objects is that the stellar bodies have their own atmosphere from which the outflowing mass is ejected out. On the other hand, compact objects, such as a black hole or a neutron star, do not have atmosphere of their own and wind must be generated from the inflow only. Given that the accretion disks surrounding them are sufficiently hot (near the inner edge) to be ionized in general, similar method as employed in stellar atmosphere could be applicable to the compact objects. Our approach in this work is precisely this. We first determine the properties of the rotating inflow and outflow and identify solutions to connect them. In this manner we self-consistently determine the mass outflow rates. In case of quasi-spherical accretion with almost zero angular momentum, the accretion disk does not form. There the pressure of pair plasma creates the virtual boundary layer which mimics the stellar atmosphere for our purpose.

Before we present our results, we describe basic properties of the rotating inflow and outflow. A rotating inflow with a specific angular momentum λ entering into a black hole will have angular momentum $\lambda \sim \text{constant}$ close to the black hole for any moderate viscous stress. This is because the viscous time scale is generally much longer compared to the infall time scale. Almost constant angular momentum produces a very strong centrifugal force λ^2/r^3 which increases much faster compared to the gravitational force $\sim GM/r^2$ and becomes comparable at around $r \sim l^2/GM$, or, $x_{cb} \sim 2\lambda^2$ where x and λ are r and l , written in units of $R_g = 2GM/c^2$ and $R_{gc} = 2GM/c$ respectively. The subscript *cb* under x stands for the centrifugal barrier. Here, (actually a little farther out, due to thermal pressure) matter starts piling up and produces the centrifugal pressure supported boundary layer (CENBOL). Farther close to the black hole, the gravity always wins and matter enters the horizon supersonically after passing through a sonic point. CENBOL may or may not have a sharp boundary, depending on whether standing shocks form or not. Generally speaking, in a polytropic flow, if the polytropic index $\gamma > 1.5$, then shocks do not form and if $\gamma < 1.5$, only a region of the parameter space forms the shock [12]. In any case, the CENBOL forms. In this region the flow becomes hotter and denser and for all practical purposes behaves as the stellar atmosphere so far as the formation of outflows

are concerned. Inflows on neutron stars behave similarly, except that the ‘hard-surface’ inner boundary condition dictates that the flow remain subsonic between the CENBOL and the surface rather than becoming supersonic as in the case of a black hole. In case where the shock does not form, regions around pressure maximum achieved just outside the inner sonic point would also drive the flow outwards. Outflow rates from accretion disks around black holes and neutron stars must be related to the properties of CENBOL which in turn, depend on the inflow parameters. Subsonic outflows originating from CENBOL would pass through sonic points and reach far distances as in wind solutions. The following 3d cartoon diagram shows the schematic geometry of the disk-jet system. The arrows show the axis of the whirling jet, D(K) stands for the Keplarian part of the disk and D(SK) stands for the subkeplarian part. CENBOL forms somewhere inside the D(SK) and J stands for the jet structure.



Geometry of the disk-jet system

Considering the inflow to be polytropic, we explore both the polytropic and the isothermal outflow. After defining the mass outflow rate as

$$\frac{\dot{M}_{out}}{\dot{M}_{in}} = R_{in},$$

We calculate this rate as a function of the inflow parameters, such as specific energy and angular momentum, accretion rate, polytropic index etc. A detail report of this work is presented elsewhere [10]. In the absence of accretion disks (inflow with almost zero angular momentum), the freely falling matter onto compact objects becomes supersonic after crossing the sonic point and may produce a standing collisionless shock due to the plasma instabilities and the nonlinearity introduced in the flow due to density perturbation [11]. Once the shock is formed, the relativistic protons provide the necessary pressure to support the shock. This

standoff shock layer then acts as the CENBOL to produce outflows for the quasi-spherical bondi type models of AGNs.

The plan of this paper is what follows: In the next section, we describe our model (when disks are formed) and present the governing equations for the inflow and outflow along with the simultaneous solution procedure. In §2, we present the results of our computation. In §3, we will discuss about the mass outflow from accretion with almost zero angular momentum (bondi type accretion) and present the schematic results. Finally, in §4, we draw our conclusions.

1 Model Description, Governing Equations and the solution Procedure

We consider thin, axisymmetric polytropic inflows in vertical equilibrium (otherwise known as 1.5 dimensional flow). We ignore the self-gravity of the flow and viscosity is assumed to be significant only at the shock so that entropy is generated. We do the calculations using Paczyński-Wiita potential which mimics surroundings of the Schwarzschild black hole. The equations (in dimensionless units) governing the inflow are:

$$\mathcal{E} = \frac{u_e^2}{2} + na_e^2 + \frac{\lambda^2}{2r^2} - \frac{1}{2(r-1)}. \quad (1)$$

$$\dot{M}_{in} = u_e \rho_e r h_e(r), \quad (2)$$

(For detail, see [12]) The equations governing the polytropic outflow are

$$\mathcal{E} = \frac{\vartheta^2}{2} + n'a_e^2 + \frac{\lambda^2}{2r_m^2(r)} - \frac{1}{2(r-1)} \quad (3)$$

$$\dot{M}_{out} = \rho \vartheta \mathcal{A}(r). \quad (4)$$

Where r_m is the mean axial distance of the flow and $\mathcal{A}(r)$ is the cross sectional area through which mass is flowing out. (For detail, see, [10]) γ of the outflow was taken to be smaller than that of the inflow because of momentum deposition effects. The outflow angular momentum λ is chosen to be the same as in the inflow, i.e., no viscous dissipation is assumed to be present in the inner region of the flow close to a black hole. Considering that viscous time scales are longer compared to the inflow time scale, it may be a good assumption in the disk, but it may not be a very strong assumption for the outflows which are slow prior to the acceleration and are therefore, prone to viscous transport of angular momentum. Detailed study of the outflow rates in presence of viscosity and magnetic field is in progress and would be presented elsewhere. The Isothermal outflow is governed

by the following equations

$$\frac{\vartheta_{iso}^2}{2} + C_s^2 \ln \rho + \frac{\lambda^2}{2r_m(r)^2} - \frac{1}{2(r-1)} = \text{Constant} \quad (5)$$

$$\dot{M}_{out} = \rho \vartheta_{iso} \mathcal{A}(r). \quad (6)$$

Here, the area function remains the same above. A subscript *iso* of velocity ϑ is kept to distinguish from the velocity in the polytropic case. This is to indicate the velocities are measured here using completely different assumptions. For details, see [10].

In both the models of the outflow, we assume that the flow is primarily radial. Thus the θ -component of the velocity is ignored ($\vartheta_\theta \ll \vartheta$).

1.1 Procedure to solve for disks and outflows simultaneously

For polytropic outflows, we solve equations (1-4) simultaneously using numerical techniques (for detail, see, [10]). In this case the specific energy \mathcal{E} is assumed to remain fixed throughout the flow trajectory as it moves from the disk to the jet. At the shock, entropy is generated and hence the outflow is of higher entropy for the same specific energy.

A supply of parameters \mathcal{E} , λ , γ and γ_o makes a self-consistent computation of R_{in} possible when the shock is present. In the case where the shocks do not form, the procedure is a bit different. It is assumed that the maximum amount of matter comes out from the place of the disk where the thermal pressure of the inflow attains its maximum and the outflow is assumed to have the same quasi-conical shape with annular cross-section $\mathcal{A}(r)$ between the funnel wall and the centrifugal barrier as already defined. For this case, the compression ratio of the gas at the pressure maximum between the inflow and outflow R_{comp} is supplied as a free parameter, since it may be otherwise very difficult to compute satisfactorily. In the presence of shocks, such problems do not arise as the compression ratio is obtained self-consistently. For isothermal outflow, it is assumed that the outflow has exactly the *same* temperature as that of the post-shock flow, but the energy is not conserved as matter goes from disk to the wind. The polytropic index of the inflow can vary but that of the outflow is always unity. The other assumptions and logical steps are exactly same as those of the case where the outflow is polytropic. Here we solve equations (1-2) and (5-6) simultaneously using numerical technique to get results. (For details, see, [10]).

2 Results

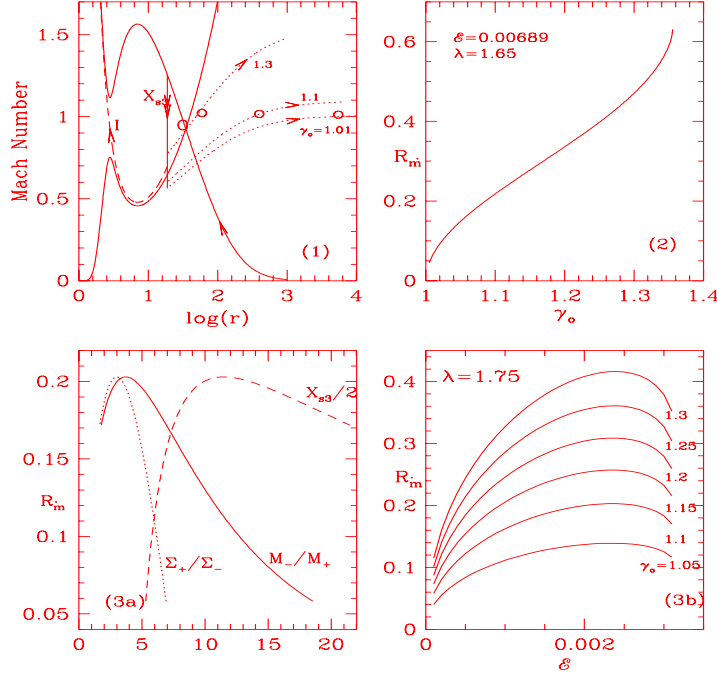


Fig. 1-3: Mach number of the flow is plotted against logarithmic radial distance both for the inflow and outflow (Fig. 1). The ratio of mass outflow rate and mass inflow rate is plotted against the polytropic index of the outflow (Fig. 2). The same ratio is plotted against the shock strength, shock location and the ratio of the integrated density (Fig. 3a) and specific energy \mathcal{E} and polytropic index of the outgoing flow γ_o (Fig. 3b). See text for details.

2.1 Polytropic outflow coming from the post-shock accretion disk

Figure 1 shows a typical solution which combines the accretion and the outflow. The input parameters are $\mathcal{E} = 0.00689$, $\lambda = 1.65$ and $\gamma = 4/3$ corresponding to relativistic inflow. The solid curve with an arrow represents the pre-shock region of the inflow and the long-dashed curve represents the post-shock inflow which enters the black hole after passing through the inner sonic point (I). The solid vertical line at X_{s3} (in the notation of [12]) with double arrow represents the shock transition. Three dotted curves represent three outflow solutions for the parameters $\gamma_o = 1.3$ (top), 1.1 (middle) and 1.03 (bottom). The outflow branches shown pass through the corresponding sonic points. It is evident from the figure that the outflow moves along solution curves which are completely different from that of the ‘wind solution’ of the inflow which passes through the outer sonic point ‘O’. The mass loss ratio R_m in these cases are 0.47, 0.22 and

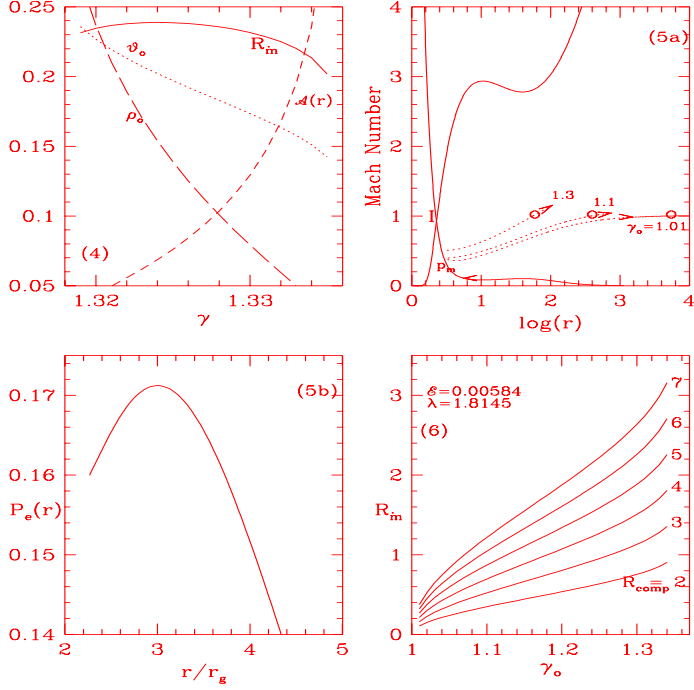


Fig. 4-6: Variation of velocity, density, cross sectional area and the rate ratio as a function of the polytropic index of the inflow (Fig. 4). Variation of the Mach number for inflow and outflow when shocks are not present (Fig. 5a). Thermal pressure variation as a function of the radial distance r/r_g showing a distinct maximum (Fig. 5b). Variation of R_{in} when both the compression ratio at the pressure maxima and polytropic index of the outflow are changed (Fig. 6). See text for details.

0.06 respectively. Figure 2 shows the ratio R_{in} as γ_o is varied. Only the range of γ_o for which the shock-solution is present is shown here. In Fig. 3a we show the variation of the ratio R_{in} of the mass outflow rate inflow rate as a function of the shock-strength (solid) M_-/M_+ (Here, M_- and M_+ are the Mach numbers of the pre- and post-shock flows respectively.), the compression ratio (dotted) Σ_+/Σ_- (Here, Σ_- and Σ_+ are the vertically integrated matter densities in the pre- and post- shock flows respectively), and the stable shock location (dashed) X_{s3} . Other parameters are $\lambda = 1.75$ and $\gamma_o = 1.1$. Note that the ratio R_{in} does not peak near the strongest shocks! Shocks are stronger when they are located closer to the black hole, i.e., for smaller energies. In Fig. 3b where R_{in} is plotted as a function of the specific energy \mathcal{E} (along x-axis) and γ_o (marked on each curve). Specific angular momentum is chosen to be $\lambda = 1.75$ as before. To have a better insight of the behavior of the outflow we plot in Fig. 4 R_{in} as a function of the polytropic index of the incoming flow γ . The range of γ shown is the

range for which shock forms in the flow. We also plot the variation of velocity ϑ_o , density ρ_o and area $\mathcal{A}(r)$ of the outflow at the location where the outflow leaves the disk. These quantities are scaled from the corresponding dimensionless units as $\vartheta_o \rightarrow 2 \times 10^4 \vartheta_o - 558$, $\rho_o \rightarrow 10^{22} \rho_o$ and $\mathcal{A} \rightarrow 0.0005 \mathcal{A}$ respectively in order to bring them in the same scale. The non-monotonic nature of the variation of $R_{\dot{m}}$ with γ is observed.

2.2 Polytropic outflow coming from the region of the maximum pressure

In this case, the inflow parameters are chosen from such a region of parameter space so that the shocks do not form (see [12]). Here, the inflow passes through the inner sonic point only. The outflow is assumed to be coming out from the regions where the polytropic inflow has maximum pressure. Figure 5a shows a typical solution. The arrowed solid curve shows the inflow and the dotted arrowed curves show the outflows for $\gamma_o = 1.3$ (top), 1.1 (middle) and 1.01 (bottom). The ratio $R_{\dot{m}}$ in these cases is given by 0.66, 0.30 and 0.09 respectively. The specific energy and angular momentum are chosen to be $\mathcal{E} = 0.00584$ and $\lambda = 1.8145$ respectively. The pressure maximum occurs outside the inner sonic point at r_m when the flow is still subsonic. Figure 5b shows the variation of thermal pressure of the flow with radial distance. The peak is clearly visible. Figure 6 shows the ratio $R_{\dot{m}}$ as a function of γ_o for various choices of the compression ratio R_{comp} of the outflowing gas at the pressure maximum: $R_{comp} = 2$ for the bottom curve and 7 for the top curve. Note that flows with highest compression ratios produce highest outflow rates, evacuating the disk which is responsible for the quiescent states in X-ray Novae systems and also in some systems with massive black holes (e.g., our own galactic centre?). The location of maximum pressure being close to the black hole, it may be very difficult to generate the outflow from this region. Thus, it is expected that the ratio $R_{\dot{m}}$ would be larger when the maximum pressure is located farther out. This is exactly what we see in Fig. 7, where we plot $R_{\dot{m}}$ against the location of the pressure maximum (solid curve). Secondly, if our guess that the outflow rate could be related to the pressure is correct, then the rate should increase as the pressure at the maximum rises. That's also what we observe in Fig. 7. We plot $R_{\dot{m}}$ as a function of the actual pressure at the pressure maximum (dotted curve). The mass loss is found to be a strongly correlated with the thermal pressure. Here we have multiplied non-dimensional thermal pressure by 1.5×10^{24} in order to bring them in the same scale.

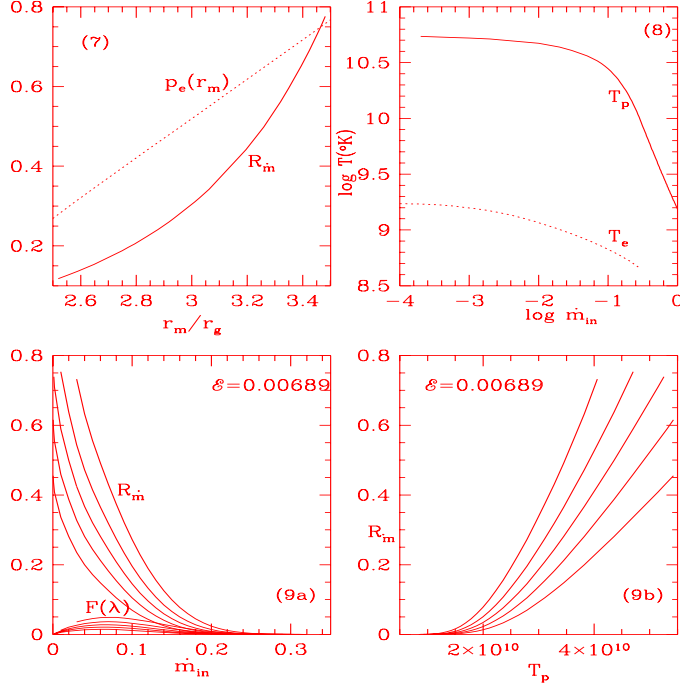


Fig. 7-9: Variation of the maximum pressure and R_m with the location where the pressure maxima occur (Fig. 7). Proton and electron temperatures in the advective region as a function of the inflow disk accretion rate \dot{m}_{in} (Fig. 8). Variation of the R_m and angular momentum flux $F(\lambda)$ as a function of the accretion rate of the inflow (Fig. 9a). Variation of R_m with proton temperature T_p (Fig. 9b). See text for details.

2.3 Isothermal outflow coming from the post-shock accretion disk

Here the temperature of the outflow is obtained from the proton temperature of the advective region of the disk. The proton temperature is obtained using the Comptonization, bremsstrahlung, inverse bremsstrahlung and Coulomb processes. [13]. Figure 8 shows the effective proton temperature and the electron temperature of the post-shock advective region as a function of the accretion rate (in logarithmic scale) of the Keplerian component of the disk. In Fig. 9a, we show the ratio R_m as a function of the Eddington rate of the incoming flow for a range of the specific angular momentum. In the low luminosity objects the ratio is larger. Angular momentum is varied from $\lambda = 1.63$ (top curve) to 1.65 (bottom curve). An interval of $\lambda = 0.005$ was used. The ratio is very sensitive to the angular momentum since it changes the shock location rapidly and therefore changes the post-shock temperature very much. We also plot the outflux of angular momentum $F(\lambda) = \lambda \dot{m}_{in} R_m$ which has a maximum at intermediate

accretion rates. In dimensional units, these quantities represent significant fractions of angular momentum of the entire disk and therefore the rotating outflow can help accretion processes. Curves are drawn for different λ as above. In Fig. 9b, we plot the variation of the ratio directly with the proton temperature of the advecting region. The outflow is clearly thermally driven. Hotter flow produces more winds as is expected. The angular momentum associated with each curve is same as before.

2.4 Isothermal outflow coming from the region of the maximum pressure

This case produces very similar result as in the above case, except that like Section 2.2 the outflow rate becomes more than a hundred percent of the inflow rate when the proton temperature is very high. This phenomenon may be responsible for producing quiescent states in some black hole candidates.

3 Poytropic outflow from quasi-spherical accretion

As already been mentioned in the introduction, for a quasi-spherical Bondi-type accretion onto a compact object (namely, on a massive black hole), a steady state situation can be developed where a standing collisionless shock may form due to the plasma instabilities and for nonlinearity introduced by small density perturbation. We consider cold inflow ($\mathcal{E} \sim 0.001$) with moderate or high value of accretion rate. Thermal particles freely falling toward black hole are assumed to be shock accelerated via first order Fermi acceleration producing relativistic protons. Those relativistic protons usually scatter several times before being captured by the black hole. These energized particles, in turn, provide sufficiently outward pressure to support a standing, collisionless shock. A fraction of the energy flux of infalling matter is assumed to be converted into radiation at the shock standoff distance through hadronic collision and mesonic decay. That fraction is radiated away to support the development and maintenance of a standing, collisionless shock at a given Schwarzschild radius. [11]

The fraction of energy converted, the shock compression ratio R_{comp} , along with the ratio of post shock relativistic hadronic pressure to infalling ram pressure at a given shock location are obtained from the steady state shock solution of Eichler [14] and Ellision and Eichler [15]. The shock location as a function of the specific energy \mathcal{E} of the infalling matter and accretion rate is then self consistently obtained using the above mentioned quantities.

We consider polytropic inflow. The outflow is also assumed to be polytropic except the fact that $\gamma_{outflow}$ is assumed to be less than the γ_{inflow} reason of which

has already been discussed in §1. As a fraction of the energy of infalling material is converted into radiation, energy flux of the wind is somewhat less than that of the accretion but is kept constant throughout the outflow. Below we present a preliminary report of the result. Detail calculation is presented elsewhere [16].

3.1 Preliminary report of the results

We solve the inflow and outflow equations self consistently as was described in §1.1 except the fact that now there will be no angular momentum related term in the energy expression and as the flow is quasi-conical, the expressions for mass flux rates are now

$$\dot{M}_{(in/out)} = \rho u r^2_{shock} \Theta_{(in/out)}$$

The value of R_{in} is distinguishably small compared to the cases previously discussed (i.e, for the rotating flows). This is because matter is ejected out due to the pressure of the relativistic particles generated at the shock location which is less enough in comparison to that originated for the presence of angular momentum. In general mass loss rate increases with the energy of the infall for fixed accretion rate. When energy is varied, mass loss rate is anti-correlated with the shock location. This is expected because higher energy gives the lower value of shock location in our model and the closer the shock forms to the black hole, the greater will be the amount of gravitational potential available to be put onto relativistic hadrons to apply pressure for the outflow to take place. If the energy is kept fixed and accretion rate is varied it is observed that the shock location increases with increasing accretion rate as expected from the functional form of the formula for calculating the shock standoff distance. Here the mass loss rate is correlated with the shock location and accretion rate. This is because once the energy is fixed, the fraction of it which is converted into radiation is also fixed implying the fact that lower is the shock location, harder is the job to produce the outflow because of the inward pull of gravity strength of which increases as the shock location decreases (for detail, see [16]).

Variation of R_{in} with the compression ratio R_{comp} at the shock location follows more or less the same trend as was manifested for the flow with angular momentum (Fig - 3a) except that here the peak is not that much distinct, and, in general, increases with the $\gamma_{outflow}$ as was seen in previous case (Fig - 2). See [16] for detail calculations and figures.

4 Concluding remarks :

In this paper, we have computed the mass outflow rate from the matter accreting onto galactic and extra-galactic black holes. Since the general physics of advective flows are similar around a neutron star, we believe that the conclusions may

remain roughly similar provided the shock forms, although the boundary layer of the neutron star, where half of the binding energy could be released, may be more luminous than that of a black hole and may thus affect the outflow rate. From numerical simulation using SPH code, it was found that the outflow rate could be as high as 10 - 20 per cent [6] which we get for moderate accretion rate and for the low value of γ_{out} . Using TVD code [8], 10 - 15 per cent of the steady outflow is seen and occasionally, even 150 per cent of the inflow is found to be driven away. Our result shows that similar high outflow rate is also possible, especially for low luminosities. Simulation for radiation dominated flows showed $R_{in} \sim 0.004$ [5], which also agrees with our results when we consider high accretion rate (see Fig. 9a). So it seems that the analytical results of our work are in good agreement with numerical simulation work. Observationally, the exact value of outflow rate from a real system is very difficult to obtain as it depends on too many uncertainties, such as filling factors and projection effects etc. In any case, with a general knowledge of the outflow rate, we can proceed to estimate several important quantities. For example, it had been argued that the composition of the disk changes due to nucleosynthesis in accretion disks around black holes and these modified isotopes are deposited in the surroundings by outflows from the disks (Hogan & Applegate 1987; Mukhopadhyay & Chakrabarti, 1998 and references therein). Similarly, it is argued that outflows deposit magnetic flux tubes from accretion disks into the surroundings (Daly & Loeb, 1990). Thus a knowledge of outflows are essential in understanding varied physical phenomena in galactic environments.

The basic conclusions of this paper (for flows with angular momentum) are the followings:

- a) It is possible that most of the outflows are coming from the centrifugally supported boundary layer (CENBOL) of the accretion disks.
- b) The outflow rate generally increases with the proton temperature of CENBOL. In other words, winds are, at least partially, thermally driven. This is reflected more strongly when the outflow is isothermal.
- c) Even though specific angular momentum of the flow increases the size of the CENBOL, and one would have expected a higher mass flux in the wind, we find that the rate of the outflow is actually anti-correlated with the λ of the inflow. On the other hand, presence of significant viscosity in CENBOL may reduce angular momentum of the outflow. When this is taken into account, we find that the rate of the outflow is correlated with λ of the outflow. This suggests that the outflow is partially centrifugally driven as well.
- d) The ratio R_{in} is generally anti-correlated with the inflow accretion rate. That is, disks of lower luminosity would produce higher R_{in} .
- e) Generally speaking, supersonic region of the inflow do not have pressure maxima. Thus, outflows emerge from the subsonic region of the inflow, whether the shock actually forms or not.

An interesting situation arises when the polytropic index of the outflow is large

and the compression ratio of the flow is also very high. In this case, the flow virtually bounces back as the winds and the outflow rate can be temporarily larger compared with the inflow rate, thereby evacuating the disk. In this range of parameters, most, if not all, of our assumptions breakdown completely because the situation becomes inherently time-dependent. It is possible that some of the black hole systems, including that in our own galactic centre, may have undergone such evacuation phase in the past and gone into quiescent phase.

So far, we made the computations around a Schwarzschild black hole. The mass outflow rates for Kerr black holes are being studied and the results would be reported elsewhere [17]. We made a few assumptions, some of which may be questionable. Nevertheless, we believe that our calculation is sufficiently illustrative and gives a direction which can be followed in the future.

REFERENCES

1. Blandford, R. D. & Payne, D. 1982, MNRAS, 199, 883
2. Chakrabarti, S. K. 1986, Apj, 303, 582
3. Chakrabarti, S. K. & Bhaskaran, P. 1992, 255, 255
4. Hawley, J.W., Smarr, L. & Wilson, J. 1984, Apj, 297, 296.
5. Eggum, G. E., Coroniti, F. V., Katz, J. I. 1985, Apj, 298, L41
6. Molteni, D., Lanzafame, G. & Chakrabarti, S. K. 1994 Apj, 425, 161
7. Nobuta, K., Hanawa, T. 1997 IAUS..184E.245N
8. Ryu, D., Chakrabarti, S. K., & Molteni, D. 1997, Apj, 474, 378
9. Castor, J. I., Abbott, D. C. & Klein, R. I. 1975, Apj, 195, 157
10. Das, T., K. & Chakrabarti, S., K. 1998 Apj, (submitted)
11. Kazanas, D. & Ellison, D. C. 1986, Apj 304, 178.
12. Chakrabarti, S. K. 1989, Apj, 347, 365
13. Chakrabarti, S. K. 1997, Apj, 484, 313
14. Eichler, D., 1984, Apj., **277**, 429
15. Ellison, D. C., & Eichler, D. 1984, Apj, **286**, 691
16. Das, T., K. 1998 (submitted)
17. Das, T., K. 1998, in preparation
18. Chakrabarti, S. K. 1997, Apj, submitted